Jurnal Kejuruteraan 32(2) 2020: 247-257
https://doi.org/10.17576/jkukm-2020-32(2)-09

Fire-Induced Flow Temperature Distribution Beneath a Ceiling

Razieh Khaksari Haddad & Mohammad Rasidi Rasani & Zambri Harun*

Faculty of Engineering & Built Environment, Universiti Kebangsaan Malaysia, Malaysia
**Corresponding author: zambri@ukm.edu.my*

Received 29 April 2019, Received in revised form 31 October 2019
Accepted 12 November 2019, Available online 30 May 2020

ABSTRACT

Many tunnels have been built to reduce traffic volumes in densely populated urban areas. In this research, a series of small-scale experiments were carried out in a 3 m length model tunnel with 0.6 m width and 0.95 m height to examine the temperature distribution along the tunnel ceiling. The containers for the source of the fire in this study were six different sizes of pools filled with n-heptane and gasoline. The smoke maximum temperature has been investigated experimentally and theoretically beneath the tunnel ceiling. A few results are obtained, firstly, dimensional analysis proposed in this research resulted in a theoretical estimation model for predicting maximum gas temperature under the ceiling. Then, the results from theoretical equation were compared with experimental data and an acceptable prediction was presented. The temperature distribution and smoke emission relationship with various ventilation velocities and heat release rate (HRR) were analyzed. The results show that an increase in ventilation velocity leads to temperature decrease and the fire source with higher HRR causes higher maximum smoke temperature. Furthermore, since the maximum temperature and the gas temperature decrease beneath the ceiling of the tunnel during the fire affect the tunnel structure, these parameters were also considered. Experimental results were also compared with that of Kurioka's model. Empirical correlations for flow temperature decay along the tunnel were also proposed based on experimental data.

Keywords: Tunnel fire management; longitudinal ventilation velocity; temperature decay empirical prediction

INTRODUCTION

The need to construct road tunnels has increased to reduce the time spent on urban travel and to increase public transport capacity and efficiency. However, several catastrophic accidents involving fires have occurred in tunnels, including 192 people killed in 2013 in the Korean Daegu Subway fire, and 40 people killed in 2014 in the Chinese Yan Hou Tunnel fire. Incidents like the above and tunnel fires also occur in the United States and Europe, where railway industries and tunnelling technologies have matured. The potential disaster arising from inadequate fire management design makes this field an important one. As a fire occurs in a tunnel, fire-induced products and hot smokes produced and diffused to a significant volume of the tunnel as they are driven in both horizontal and vertical directions by buoyancy force. Consequently, the knowledge of dominant smoke movements and fire spread patterns are essential to evacuate commuters safely, decrease the damage to tunnel structure and equipment, and provide an environment for smooth fire extinguishing and evacuation activities. As an example, an earlier study found that an existing smoke extraction system is insufficient to provide a safe evacuation from train platform in an underground train station (Harun et al. 2014).

Smoke is controlled and propagated in the opposite direction of passing vehicles by longitudinal ventilation in expressway road tunnels. *Backlayering* is the smoke return flow, which diffuses against the longitudinal ventilation flow in the distance between the fire source and ventilation fan. The minimum ventilation velocity that can eliminate the backlayering stream is called *critical velocity*. Research on the backlayering phenomenon and the critical velocity for stopping backlayering thermal fumes during a tunnel fire has been considered, a review of which could be found in Haddad et al. (2019a). Furthermore, an appropriate designs for fire detectors and fire protection services can be equipped if the temperature distribution of smoke flow under the ceiling of the tunnel is predicted accurately. Many studies have been conducted in the field of tunnel fires to investigate maximum temperature of fire-induced products along the tunnel ceiling and temperature decay through a tunnel (Yan et al. 2009; Li et al. 2011; Li et al. 2012; Ji et al. 2011).

Oka and Atkinson (1995) carried out experimental tests in which ceiling height, ventilation velocity, and fire sizes were varied and the maximum temperature of smoke beneath the ceiling of the tunnel was examined with regards to the effect of longitudinal ventilation velocity. In their study, the empirical relations for the flame tilt angle, the maximum temperature of fire-induced flow, and its position were proposed. The maximum smoke temperature was studied in Kurioka et al.

(2003) and an empirical model was extracted to compute the maximum excess gas temperature under the tunnel ceiling as follows:

$$\frac{\Delta T_{max}}{T_a} = \gamma \left(\frac{Q^{*2/3}}{Fr^{1/3}} \right)^{\varepsilon}, \tag{1}$$

where

$$\begin{cases} \gamma = 1.77, \varepsilon = 1.2 \\ \text{for } \left(\frac{Q^{*\frac{2}{3}}}{Fr^{\frac{1}{3}}} \right) < 1.35, \\ \gamma = 2.54, \varepsilon = 0 \\ \text{for } \left(\frac{Q^{*\frac{2}{3}}}{Fr^{\frac{1}{3}}} \right) \geq 1.35, \end{cases} \tag{2}$$

$$Q^* = \frac{Q}{\rho_a T_a C_p g^{1/2} H^{5/2}}, \tag{3}$$

and

$$Fr = \frac{V^2}{gH}. \tag{4}$$

However, the ratio of the maximum smoke temperature to ambient temperature becomes zero in Equation (1) while ventilation velocity reaches zero (Fr = 0). Therefore, this equation cannot provide correct results when the ventilation velocity is considerably low. Full-scale data were compared with Equation (1) in Hu et al. (2005). Although good agreement was observed between them, the measured maximum ceiling temperatures were lower than the values estimated by Equation (1) because lower heat release rates (HRRs) were used.

The maximum smoke temperature when the distance between the fire source and the vertical walls was 1.8 times longer than the tunnel height was investigated in Alpert (1972). The following expression was derived:

$$\Delta T_{max} = 16.9 \frac{\dot{Q}^{2/3}}{H^{5/3}}, \qquad H < 0.18. \tag{5}$$

Further, the maximum temperature of fire-induce flow was estimated in Li et al. (2011) found on scaled experimental results and analysis.

$$\Delta T_{max} = \begin{cases} \frac{Q}{ur^{\frac{1}{3}} H_d^{\frac{5}{3}}} & \text{for } u' > 0.19, \\ \frac{17.5Q}{H_d^{5/3}} & \text{for } u' \leq 0.19, \end{cases} \tag{6}$$

where

$$u' = {}^{u}/_{u^*}, \tag{7}$$

and

$$u^* = \left(\frac{Q_c g}{r \rho_a C_p T_a} \right)^{1/3}. \tag{8}$$

The calculation of temperature at each point depends on the maximum temperature and the temperature reduction relative to the distance from the source of the fire. Hu et al. (2005) derived the exponential relationship of gas temperature decay along a tunnel as follows:

$$\frac{\Delta T_x}{\Delta T_0} = \frac{T_x - T_0}{T_0 - T_a} = \exp k(x - x_0), \tag{9}$$

where

$$k = \frac{\alpha D}{C_p \dot{m}}. \tag{10}$$

Temperature distribution in a tunnel was studied by Zhao et al. (2018) in this experiment both ventilation velocity and fire size were changed. The influence of varying ventilation velocity and HRR on the temperature distribution was influenced and a modified coefficient that was related to the longitudinal velocity and HRR was presented for the upstream temperature decay equation. It is also concluded that the temperature distribution in the downstream, ventilation velocity has a more significant effect on the smoke temperature disposal at the downstream section. Tang et al. (2019) carried out a series of small-scale experiments and investigated the maximum temperature induced by carriage fire in a tunnel with smoke extraction.

The variables in Tang's study; ceiling smoke extraction rate and heat release rate and maximum smoke temperature beneath the ceiling were analyzed with regard to ceiling smoke extraction. Tang et al. (2019) proposed a correlation between maximum temperature of smoke and its extraction rate.

In this research, small-scale experiments were executed in a 3 m scaled tunnel. Eight longitudinal points along the ceiling of the tunnel were selected to measure smoke temperature. In addition to the effect of the variation of longitudinal ventilation velocities and HRRs on the smoke temperature, the maximum temperature of smoke and temperature decay beneath the ceiling were also examined. Furthermore, the maximum smoke temperature in a longitudinal ventilated tunnel was analysed theoretically by the Ipsen method (Ipsen, 1960) and

a model was proposed to predict the maximum temperature of hot gases based on fundamental dimensions of influencing parameters.

EXPERIMENTAL SETUP

Model tunnel

Figure 1 shows the side view of the model tunnel. The scaled model, which is a 1:50 scale of the Resalat Tunnel, was constructed based on the Froud scaling model (Heskestad, 1973; Quintiere, 1989). The 150-meter Resalat Expressway connects the east-west of Tehran, Iran. This tunnel connects Seyed Khandan in north-central Tehran to the western parts of Greater Tehran. According to the length of the Resalat model and chosen scale, the length of the tunnel, *L*, is scaled geometrically. The fire source was positioned in the origin of the coordinates, at a distance of 164 cm from the right end of the tunnel. The studied model has a length of 3 m (*x* coordinate), a width of 0.6 m (*y* coordinate), and a height of 0.95 m (*z* coordinate). The cross section of the model tunnel is rectangular. Fireproof boards with 25 mm thickness were used to construct the sidewalls and the ceiling of the tunnel. Ceramic oxide and silicon dioxide are the components of fireproof boards which make together thermal conductivity within the range of 0.1-0.14 W/mK. Using tempered glass in one of the sidewalls allows the observation of the smoke movement.

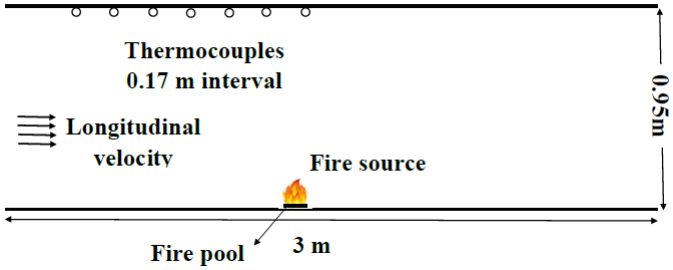

FIGURE 1. The cross-section view of the model tunnel

Measurement

Measurement devices for detecting backlayering flow and temperature disperse in the upstream section were bare thermocouples (K-type, 0.3 mm in diameter), which was installed in the horizontal direction inside the tunnel. Continuous measurements as well as adequate results in the range of -250 °C to 1260 °C is obtained by a K-type thermocouple. Ambient temperature was approximately 27 °C -28 °C in all experiments. The positions of eight thermocouples were 1 cm below the tunnel ceiling with 0.17 m intervals. Measurement response time was 1 s. Temperature measurement was calibrated before starting the tests. Figure 1 shows the length at which the smoke temperature is measured from 0 to 1.35 m. Arduino MEGA 2560 was configured as a data acquisition device. A three-phase ventilation fan with a power of 400 W and an airflow capacity of 5700 m^3/h was installed at the left end of the tunnel to attain longitudinal ventilation flow. The ventilation velocity was controlled by varying the voltage through the Toshiba frequency inverter VF-S11. The relationship between various inverter frequencies and velocity inside the tunnel was derived and then different velocities in experiments were calculated by this relationship.

Since the airflow should be roughly laminar and homogeneous throughout the test section to increase the accuracy of measurements, one honeycomb mesh, and two wire mesh screens were connected between the ventilation fan and the main model tunnel. This equipment straightens the ventilation flow as axial turbulence reduced more than lateral turbulence by screens. Mehta and Bradshaw (1979) proved that multiple screens with a comparably high open area ratio ($\beta > 0.58$) in series arrangements lead to anoptimum turbulence reduction. Therefore, a coarse screen with a 1 mm size and a fine screen with 0.5 mm were used in this study. The adequate space between screens is 500 wire diameters as suggested in Barlowlow et al. (1999), 250 mm for the standard 0.5 mm-diameter wire in this experiment. Slight pressure is reduced by honeycomb mesh which influences axial velocities and reduces lateral velocities. Mehta and Bradshaw (1979) also proposed that the length of the cell in honeycomb mesh should be about 6–8 times its diameter. This issue led to utilize a pipe length of 7 cm for the pipe diameter of 1.11 cm, which provides an aspect ratio of 6.5. The distance between the honeycomb mesh and the metal screens was considered longer than 30 times the mesh size as Growth & Johansson (1988) recommended.

Six different square pools filled with n-heptane (C_7H_{16}) and gasoline (C_8H_{18}) were used to perform reduced-scale experiments. The lengths of polls were 0.08, 0.1, 0.12, 0.15, 0.18, and 0.21 m, which produced fires between 2.21 and 34.55 kW, respectively. The approximate fire sizes in a tunnel with a diameter of 5.13 m (the Resalat tunnel diameter), which these pool dimensions correspond to, are 39-610 MW when the Froude scaling model was used. One centimeter of 2 cm depth of each pool was filled with fuel.

The parameter which determines the HRR is fuel weight loss. The HRR was determined by the rate of fuel mass loss ($\dot{m}_f$) using the following equation:

$$Q = \dot{m}_f \aleph H_T, \tag{11}$$

and

$$\dot{m}_f = \dot{m}_\infty (1 - e^{-k\theta}). \tag{12}$$

The values used for n-heptane are as follows:

$$\begin{cases} \dot{m}_\infty = 0.101 \frac{\text{kg}}{\text{m}^2\text{s}}, \\ H_T = 44.6 \frac{\text{Mj}}{\text{kg}}, \\ k\theta = 1.1\ \text{m}^{-1} \end{cases} \tag{13}$$

Experimental procedure

A series of 77 experimental tests were conducted in this study. Subjects that have been sought out are the influence of various ventilation velocities and HRRs on temperature distribution, maximum smoke temperature, and gas temperature decay.

Uncertainties of the model approach and measurement system

Scaling

The modeling of the smoke flow and the recreation of both inertial and buoyancy forces were performed in a reduced–scale tunnel structure with a 1:50 scale. The preservation of the aforementioned numbers, which are Froude and Richardson numbers, will be hardly achieved because of the small scale used. However, the same trend and a sufficient agreement between the derived results and correlations from references show the minor impact of the scale size.

Heat release rate

The conductive heat transfer has the main effect on the total amount of heat transferring from smoke to tunnel walls. This type of heat transfer varies with HRR, distance to the fire source, tunnel dimensions, and materials. Since there were differences between the thickness and thermal properties of the full–scale tunnel and the model ones (fireproof board and tempered glass walls), more heat is wasted via the model sidewalls and its ceiling in comparison with the full-scale tunnel. For example, an increase in the heat loss, especially around the fire source, is predictable due to using the tempered glass fixed in the half of one sidewall. Consequently, the thermal phenomena from the full–scale fire size cannot be reproduced equitably by the isothermal model in this study. Moreover, the calculation of HRR can cause uncertainties as for heptane and gasoline heat properties were collected theoretically from Babrauskas (1983) which leads to slight differences compared with the actual values.

Measuring system

There are sources of error related to measuring devices that may affect the results. In this research, the measurement uncertainties of devices were calculated through calibration, the manual provided by the manufacturer, and from references. Thermocouples have been selected to measure temperature because of their ease of use and their functionality. The data acquisition system included thermocouples, Arduino MEGA 2560, and amplifier MAX6675K. Therefore, the uncertainties of all elements in the temperature measurement chain should be considered by estimating and recording the measurement errors of the temperature. Regarding thermocouples, the response to thermal changes, radiation impact, and conduction heat transfer by the wire influence the accuracy of temperature measurement. The error value of conduction heat transfer was estimated by comparing the temperature measured by the thermocouple with twisted wire and the thermocouple with not twisted wire, which was 2% and 5% respectively. The uncertainties created through radiation is insignificant in a high-temperature region in a building fire (Luo, 1997), although its impact cannot be completely ignored. The uncertainties related to radiation heating and cooling can be decreased if smaller diameter thermocouples were utilized (Walker and Stocks, 1968). The temperature recorded by a K-type thermocouple then delivered to amplifier MAX6675K. Amplifier MAX6675K digitizes the signal and provides a microcontroller compatible digital serial interface. Based on the information provided in the MAX6675K manual, the error related to amplifier MAX6675K is 0.29% in temperatures between 0 °C and +700 °C. Arduino MEGA 2560, which is the data acquisition instrument, has an accuracy of ±2 LSB in measuring voltages. Therefore, for a 10 bit-system, the maximum error was 2 bits (1024 decimal, 0.25%). These errors are described in Table 1:

TABLE 1. Uncertainty estimates

Source	Uncertainty
Thermocouples	2%
Arduino MEGA 2560	0.25%
Amplifier MAX6673K	0.29%
Wire	1.5%

MAXIMUM SMOKE TEMPERATURE DIMENSIONAL INVESTIGATION BENEATH THE CEILING

Parameters that influence maximum smoke temperature are heat release rate, ventilation velocity, tunnel height, and ambient properties. In this section, non–dimensional parameters are utilized. All significant and effective values which are the maximum smoke temperature of fire–induced flow beneath the ceiling are proposed by a dimensionless model. The influencing factors are chosen based on previous research results e.g. Li et al. (2011) and Haddad et al. (2019b). A general relationship for the maximum smoke temperature under the tunnel ceiling is as following:

$$\emptyset\left(\Delta T_{max}, T_a, Q, \rho, C_p, g, u, H_d\right) = 0. \quad (14)$$

Fundamental dimension of weight, time, temperature, and length are assigned by [M], [t], [T] and [L]. Therefore, the above function is expressed by the corresponding dimension equation below:

$$\emptyset\begin{pmatrix} T, T, ML^2t^{-3}, ML^{-3}, L^2t^{-2}T^{-1}, \\ Lt^{-2}, Lt^{-1}, L \end{pmatrix} = 0. \quad (15)$$

The main dimension of the above equation is simplified by the Ipsen method (Ipsen, 1960). ρ is selected to remove [M] and a simplified equation is obtained as follows:

$$\emptyset(T, T, L^5t^{-3}, L^2t^{-2}T^{-1}, Lt^{-2}, Lt^{-1}, L) = 0, \quad (16)$$

$$\emptyset\left(\Delta T_{max}, T_a, \frac{Q}{\rho}, C_p, g, u, H_d\right) = 0. \quad (17)$$

H_d is elected to remove [L] and a new relationship is introduced as follow:

$$\emptyset(T, T, t^{-3}, t^{-2}T^{-1}, t^{-2}, t^{-1}) = 0, \quad (18)$$

$$\emptyset\left(\Delta T_{max}, T_a, \frac{Q}{\rho H_d^5}, \frac{C_p}{H_d^2}, \frac{g}{H_d}, \frac{u}{H_d}\right) = 0. \quad (19)$$

g is selected to remove [t] and a new mathematic expression is derived as follow:

$$\emptyset(T, T, T^{-1}) = 0. \quad (20)$$

$$\emptyset\left(\Delta T_{max}, T_a, \frac{QH_d^{3/2}}{\rho H_d^5 g^{3/2}}, \frac{C_p}{H_d g}, \frac{u}{H_d^{1/2} g^{1/2}}\right) = 0. \quad (21)$$

Finally, [T] was eliminated by T_a and a new equation is obtained i.e.:

$$\emptyset\left(\frac{\Delta T_{max}}{T_a}, \frac{Q}{\rho H_d^{7/2} g^{3/2}}, \frac{C_p T_a}{H_d g}, \frac{u}{H_d^{1/2} g^{1/2}}\right) = 0. \quad (22)$$

Which is simplified as follows:

$$\emptyset\left(\frac{\Delta T_{max}}{T_a}, \frac{Q}{\rho u H_d^3 g}, \frac{C_p T_a}{H_d g}\right) = 0, \quad (23)$$

where $F_Q = \frac{Q}{\rho u H_d^3 g}$ and $F_T = \frac{C_p T_a}{H_d g}$.

The dimensionless power equation which calculate the smoke maximum temperature is as follows:

$$\frac{\Delta T_{max}}{T_a} = k_1 F_Q^{k_2} F_T^{k_3}. \quad (24)$$

The correlation coefficient should be derived based on the experiment results. Firstly, both sides of the equation are transferred into a multivariate linear problem with the logarithmic method.

$$\mathrm{Ln}\left(\frac{\Delta T_{max}}{T_a}\right) = \ln(k_1) + k_2 \ln\left(F_Q\right) + k_3 \ln(F_T). \quad (25)$$

The GNU Octave package, which is a high-level programming language, mostly designed for numerical calculation, is chosen to calculate equations of 77 experimental results and determine the coefficients. Then, substituting the coefficients of k_1, k_2, and k_3 into Equation (25) and the best group of coefficients is chosen, which gives 0.85 fitting correlation coefficient as follows:

$$R^2 = 1 - \frac{\sum(y_i - f_i)^2}{\sum(y_i - \bar{y}_i)^2}, \quad (26)$$

where y_i, $\bar{y}$ and f_i are experimental data, the mean of experimental data, and modeled values, respectively. An empirical formula was deduced to express the maximum gas temperature beneath the tunnel ceiling:

$$\ln\left(\frac{\Delta T_{max}}{T_a}\right) = 31.11 + 0.520\ln(F_Q) - 9.779\ln(F_T). \quad (27)$$

Next, substitute the experimental data for F_Q and F_T into Equation (27) and the comparison between experimental results and data derived from the empirical formula is shown in Figure 2. Investigating the fitting correlation coefficient in different speed intervals shows that the accuracy of this formula decreases at higher velocities. Therefore, a further study to derive a more accurate equation, especially for velocities more than 1.5 m/s is needed.

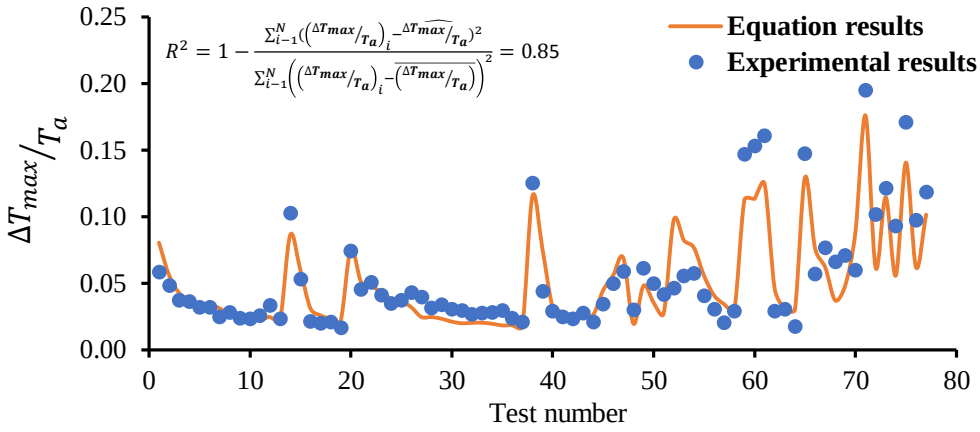

FIGURE 2. The comparison between experimental results and data derived from the empirical formula

RESULTS AND DISCUSSION

The effect of ventilation velocity in the longitudinal direction

The influence of various ventilation velocities on the maximum smoke temperatures and smoke propagation was measured for several fire sizes (2.21, 4.22, 7.12, 22.48 and 34.55 kW) at different positions through the roof. As a result of heat loss of smoke flow to the surrounding boundaries as well as ambient air, the maximum smoke temperature decreases when fire-induce flow spreads longitudinally as shown in Figure 3. Various factors affect this decline. These causes include thermal convection between hot smoke flow and the ceiling of the tunnel, heat transferred by radiation between smoke and adjacent cold air, and heat wasted due to inlet air. Heat exchange with the surrounding walls and the entrance air are enhanced with increasing longitudinal velocity. Therefore, in a situation with lower ventilation velocity, the maximum smoke temperature was higher. Moreover, in situations with smaller ventilation velocities, the smoke temperature decreased with greater intensity. Longitudinal ventilation velocity significantly influences temperature along the ceiling.

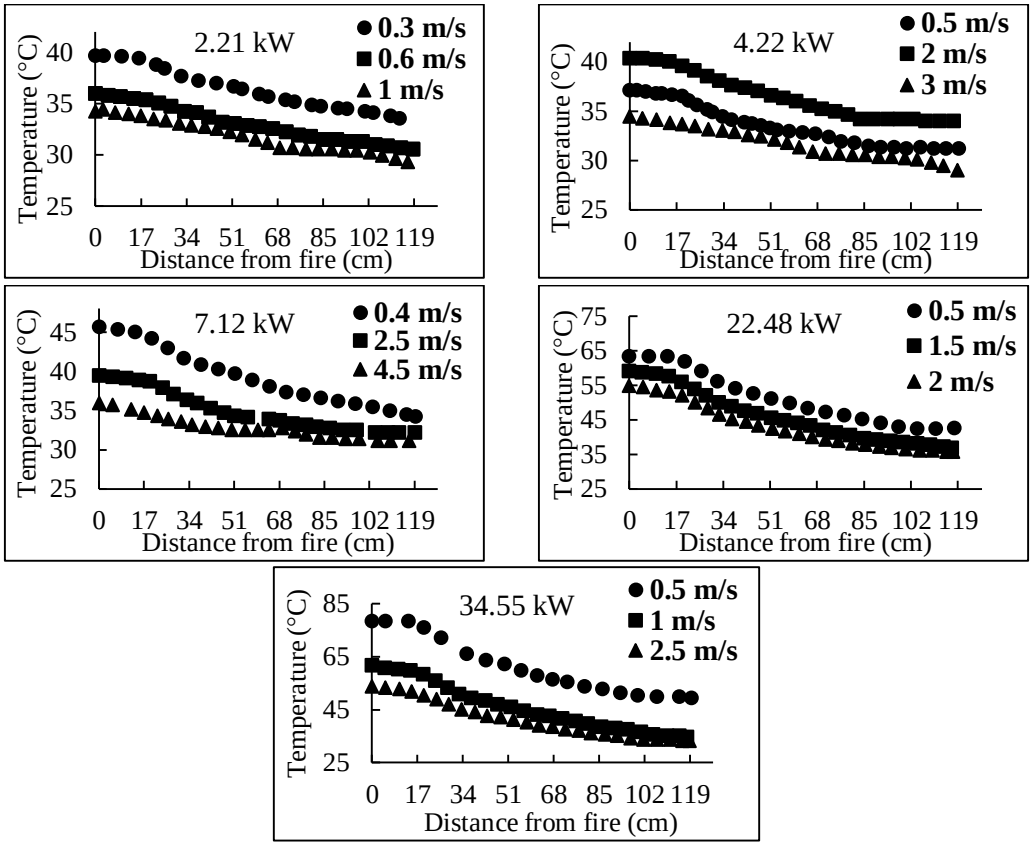

FIGURE 3. Maximum temperature changes at different ventilation velocity along the tunnel ceiling

The influence of heat release rate

In the same model tunnel, the maximum smoke temperature has subsequently experienced an increase when the fire source's size (HRR) increased. Although with the movement of the smoke along the downstream its temperature with different fire sizes declined, as shown in Figure 4. The smoke layer temperature was higher for bigger fire sizes because more HRR dispenses more heat to the surroundings. For example, the maximum smoke temperatures measured with HRR 34.55 kW were approximately 12 °C higher than that with an HRR of 13.45 kW at 1 m/s ventilation velocity. The smoke flow reached its highest temperature just above the source of the fire, and then the temperature of fire-induced products decreased gradually when smoke spread along the ceiling. This trend, temperature progress along the longitudinal direction, repeated for various fire sizes.

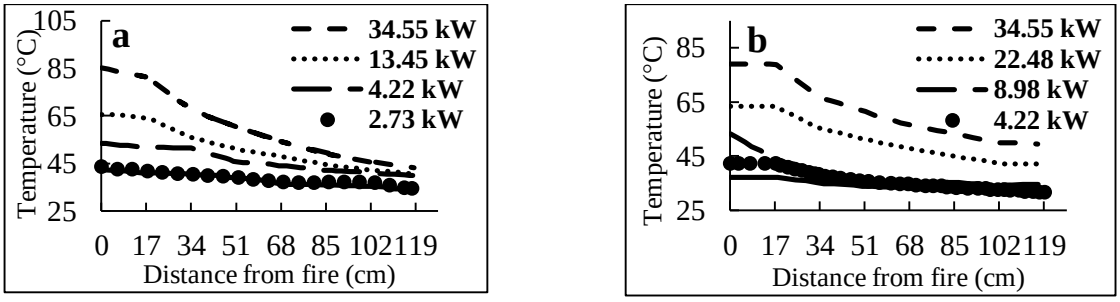

FIGURE 4. The variation of the maximum smoke temperature along the tunnel ceiling in relation to different heat release rate at 1 m/s (a) and 0.5 m/s (b).

Maximum temperature of the smoke layer under the tunnel ceiling

When a fire occurs in the tunnel, the maximum temperature of fire-induced flow is a significant parameter that should be considered in the designing of the tunnel structure and the evaluation of the tunnel ceiling material performance. The parameters whose impact should be considered in the maximum temperature estimation in a longitudinally ventilated tunnel are ventilation velocity in the longitudinal direction, HRR, ambient properties, tunnel effective height, and gravitational acceleration (Li et al. 2011; Kurioka et al. 2003). Therefore, in this experiment, the maximum temperature obtained from experimental results were plotted based on two non-dimensional parameters, $\Delta T_{max}/\Delta T_a$ and $Q^{*2/3}/Fr^{1/3}$. Parameter $Q^{*2/3}/Fr^{1/3}$ was selected to encompass the impact of all the mentioned parameters. As indicated in previous sections, the maximum smoke temperature changes are directly related to HRR and have an indirect relationship with the longitudinal ventilation velocity. The fire sizes in this experiment were 2.21-34.55 kW at various ventilation velocities. The results, along with the first part of the empirical equation in Kurioka et al. (2003) were presented in Figure 5.

The experimental results agree well with the calculation of the power equation in Kurioka et al. (2003) (i.e. only the coefficient A and the power B are different in the equation $A \times \left(Q^{*2/3}/Fr^{1/3}\right)^{B}$. Nevertheless, the comparison between our experimental data and Kurioka's results (Kurioka et al., 2003) displays that Kurioka's model overestimates the maximum gas temperature. The reason for this is the use of thick fireproof boards at the ceiling of the tunnel in Kurioka's model, which can lead to an improper prediction of maximum temperature and overestimating the maximum excess temperature of the smoke. Furthermore, the fire is closer to the sidewall when the tunnel height is taller than the tunnel width, the aspect ratio is less than 1. This issue indicates that the fire flow is different in a tunnel with an aspect ratio of less than 1 examined with the condition in which the tunnel height is larger than its width due to the restricting impact of sidewalls on the fire plume dispersion. Consequently, the maximum temperature of smoke beneath the tunnel ceiling will have smaller values. The data can be closely presented by a power fitting trend line (Equation (28)). That is when $Q^{*2/3}/Fr^{1/3} <$ 1.35, the relationship between the maximum temperature below the ceiling and $Q^{*2/3}/Fr^{1/3}$ can be defined by an exponential equation to approximately 4/5 power of $Q^{*2/3}/Fr^{1/3}$ as follows:

$$\frac{\Delta T_{max}}{\Delta T_a} = 0.413\left(Q^{*2/3}/Fr^{1/3}\right)^{0.853}. \quad (28)$$

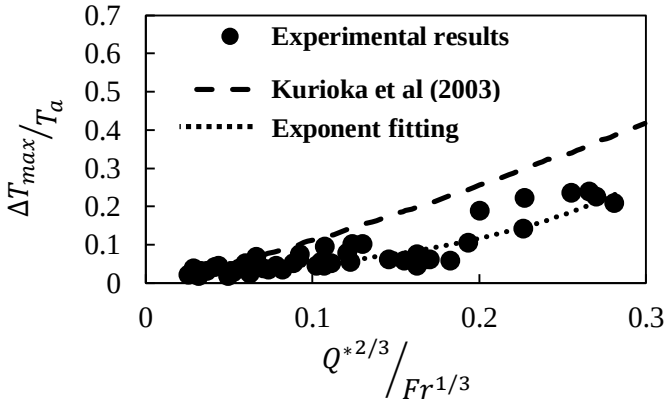

FIGURE 5. The maximum excess gas temperature beneath the ceiling of the tunnel against $Q^{*2/3}/Fr^{1/3}$

Smoke temperature decay beneath the tunnel ceiling

The estimation of the temperature of the smoke layer at any point along the ceiling of the tunnel is related to the maximum smoke temperature and the relationship between the temperature reduction ratio and the measuring point position relative to the source of fire (Hu et al. 2013). In a tunnel fire, the heat that is wasted by convection through the surrounding walls and the radiation heat which is lost by combining with ambient air and the

boundaries have a significant influence on smoke temperature decay. The relationship between the non-dimensional temperature dispensation through the tunnel ceiling ($^{\Delta T_x}/_{\Delta T_a}$) for six fire sizes and the dimensionless downstream distance to the fire source (*x/H*) was drawn in Figure 6 to present the smoke temperature propagation through the longitudinal direction. Overall, the temperature trend along the tunnel ceiling exhibits an exponential decay, which agrees with the theoretical and experimental results proposed in the literature. However, the dimensionless temperature is reduced when the distance between the measurement point and the fire source is increased, which demonstrates that the smoke flow shape belongs to the 1D spreading phase. In Figure 6(b), when the fire source is 8.98 kW and velocity is 2.8 m/s, the dimensionless temperature rise is 0.686 at x = 0.68 m while it is 0.523 at x = 1.02 m. Another example is for 22.48 kW at 0.5 m/s velocity (Figure 6(e)) where the dimensionless temperature is 0.660 and the distance from the fire source is 0.68 m whereas it is 0.493 at x = 1.02 m. The exponential fitting equation for each fire size is listed in Table 2:

TABLE 2. The experimental fitting equation list for all fire sizes

Pool No.	Fuel	The rate of Heat release (kW)	Fitting equation	R^2
1	n-heptane	2.73	$^{\Delta T_x}/_{\Delta T_a} = 0.9363e^{-0.6614x}$	0.899
2	n-heptane	5.26	$^{\Delta T_x}/_{\Delta T_a} = 1.017e^{-0.7624x}$	0.967
3	n-heptane	8.98	$^{\Delta T_x}/_{\Delta T_a} = 0.914e^{-0.6x}$	0.899
4	Gasoline	13.43	$^{\Delta T_x}/_{\Delta T_a} = 1.023e^{-0.793x}$	0.983
5	Gasoline	22.48	$^{\Delta T_x}/_{\Delta T_a} = 1.022e^{-0.764x}$	0.979
6	Gasoline	34.55	$^{\Delta T_x}/_{\Delta T_a} = 1.026e^{-0.768x}$	0.980

From the preceding investigation, a fitted relationship with $R^2 = 0.92$ is obtained to measure the smoke temperature along the ceiling at any interval from the fire source:

$$\frac{\Delta T_x}{\Delta T_a} = \frac{T_x - T_a}{T_0 - T_a} = 0.990e^{-0.725x}. \quad (29)$$

According to Hu et al. (2005), the equation for the dimensionless temperature increase ($^{\Delta T_x}/_{\Delta T_a}$) based on distance from where the fire source is placed for slope 0 % is as follows:

$$\frac{\Delta T_x}{\Delta T_a} = 1.003e^{-0.35x}. \quad (30)$$

The comparison between the equation derived from the results of this study (Equation (29)) and the equation in Hu et al. (2005) shows that despite different coefficients, they agree with each other due to exponential trend. The essential cause of the difference is varying experimental conditions that lead to different temperature decay equations because heat loss through the walls as well as the length limitation of the current model, which causes *stack effect*, influence the temperature decay.

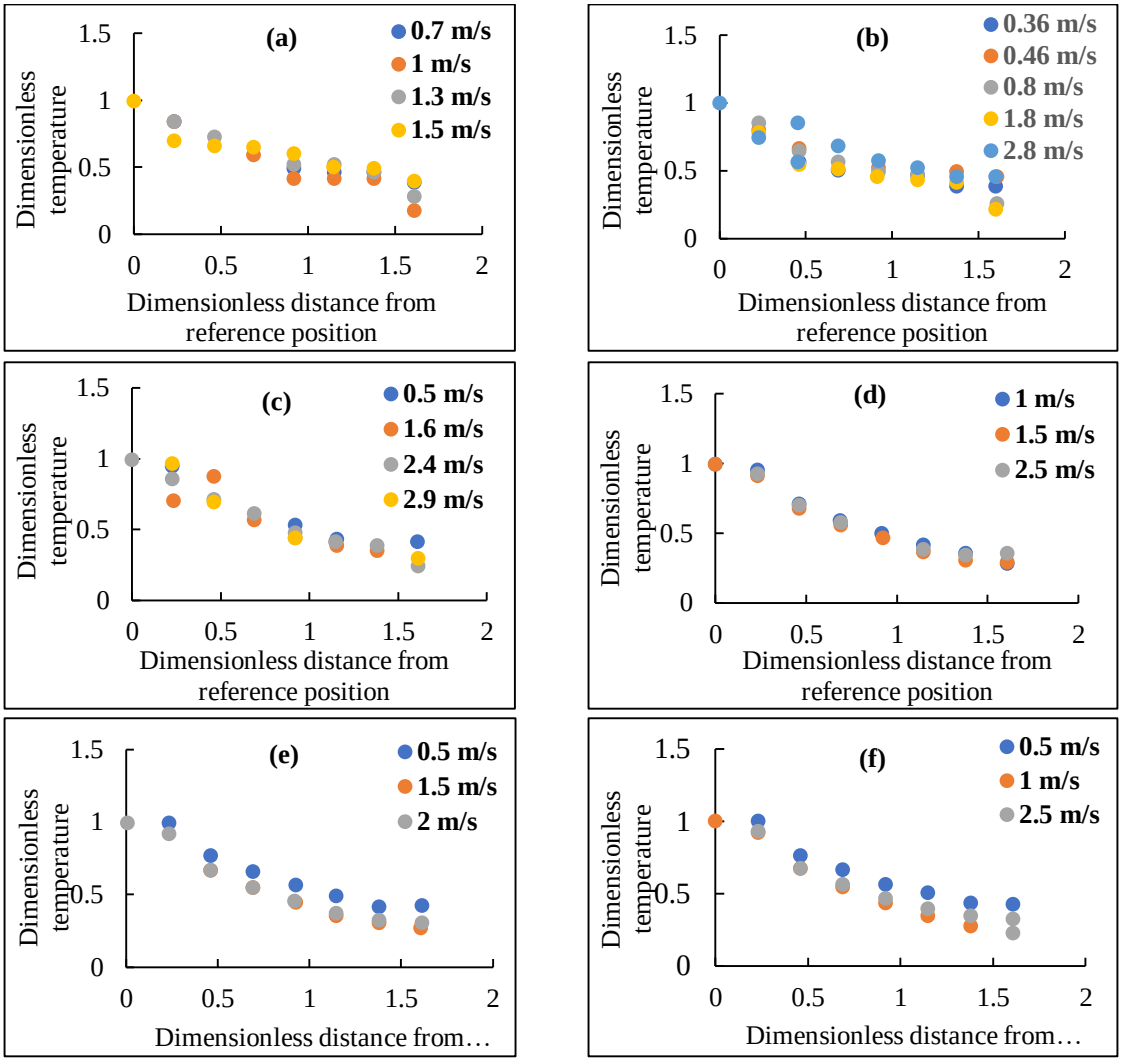

FIGURE 6. The dimensionless temperature distribution versus dimensionless distance downstream from the origin for different heat release rates as follows: (a) 2.73 kW, (b) 8.98 kW, (c) 4.22 kW, (d) 13.42 kW, (e) 22.48 kW, and (f) 34.55 kW

CONCLUSION

The smoke temperature along the ceiling of the tunnel was examined by a small-scaled experimental tunnel fire study. Different HRRs and longitudinal ventilation velocities are considered in this study.

The main outlines of the experimental results of this study are:

- Ventilation velocity variations influence the smoke temperature distribution in the section between the left end of the tunnel and the origin. The temperature of the fire-induced products decreases with increasing ventilation velocity, although lower temperature decay observed in these conditions.
- The higher smoke temperature under the tunnel ceiling is a result of a bigger fire size with higher HRR. Although the temperature of bigger fire source products declines faster whilst moving along the tunnel.
- An empirical equation is proposed based on a dimensionless technique, which can estimate ΔT_{max} with a 0.85 fitting correlation coefficient.
- Also, the maximum excess gas temperature changes with about 4/5 power of $Q^{*2/3}/Fr^{1/3}$ when $Q^{*2/3}/Fr^{1/3}$<1.35. The experimental results of ΔT_{max} are also compared with those in Kurioka et al. (2003). The coefficient of our equation varies from that in Kurioka et al. (2003) because of differences in fire size and geometric conditions.
- The dimensionless temperature increases when smoke spreads over the tunnel ceiling can be determined by an exponential decay

for all experiments as predicted in Hu et al. (2013). However, due to dissimilar experimental environments, the coefficients are different.

ACKNOWLEDGEMENT

We are grateful for the financial assistance provided by the FRGS/1/2016/TK03/UKM/03/1 grant from the Ministry of Education Malaysia (MOE) and UKM grant GUP-2018-102.

REFERENCES

Alpert, R. L. 1972. Calculation of response time of ceiling-mounted fire detectors. *Fire Technology* 8(3): 181-195.

Babrauskas, V. 1983. Estimating large pool fire burning rates. *Fire Technology* 19(4): 251-261.

Barlow, J. B., Rae, W. H., & Pope, A. 1999. Low-speed wind tunnel testing.

Groth, J., & Johansson, A. V. 1988. Turbulence reduction by screens. *Journal of Fluid Mechanics* 197: 139-155.

Heskestad, C. 1973. Modeling of enclosure fires. *In Symposium (International) on Combustion* 14(1): 1021-1030.

Hu, L. H., Chen, L. F., Wu, L., Li, Y. F., Zhang, J. Y., & Meng, N. 2013. An experimental investigation and correlation on buoyant gas temperature below ceiling in a slopping tunnel fire. *Applied Thermal Engineering* 51(1-2): 246-254.

Hu, L. H., Huo, R., Li, Y. Z., Wang, H. B., & Chow, W. K. 2005. Full-scale burning tests on studying smoke temperature and velocity along a corridor. *Tunnelling and Underground Space Technology* 20(3): 223-229.

Ipsen, D.C., 1960. Units, dimensions, and dimensionless numbers. McGraw-Hill.

Ji, J., Zhong, W., Li, K. Y., Shen, X. B., Zhang, Y., & Huo, R. 2011. A simplified calculation method on maximum smoke temperature under the ceiling in subway station fires. *Tunnelling and Underground Space Technology* 26(3): 490-496.

Haddad, R. K., Maluk, C., Reda, E., & Harun. Z. 2019a. Critical velocity and backlayering conditions in rail tunnel fires: State-of-the-art review. *Journal of Combustion*, No. 3510245.

Haddad, R. K., Harun, Z., Maluk, Z. C., & Rasani M. R. (2019b) Experimental study of the influence of blockage on critical velocity and backlayering length in a longitudinally ventilated tunnel. *JP Journal of Heat and Mass Transfer* 17(2): 451-476.

Harun, Z., Sahari, M. S. & Mohamad, T. I. 2014. Smoke simulation in an underground train station using computational fluid dynamic, *Applied Mechanics and Materials* (663): 366–372.

Kurioka, H., Oka, Y., Satoh, H., & Sugawa, O. 2003. Fire properties in near field of square fire source with longitudinal ventilation in tunnels. *Fire Safety Journal* 38(4): 319-340.

Li, J., Liu, S., Li, Y., Chen, C., Liu, X., & Yin, C. 2012. Experimental study of smoke spread in titled urban traffic tunnels fires. *Procedia Engineering* 45: 690-694.

Li, L., Cheng, X., Wang, X., & Zhang, H. 2012. Temperature distribution of fire-induced flow along tunnels under natural ventilation. *Journal of Fire Sciences* 30(2): 122-137.

Li, Y. Z., Lei, B., & Ingason, H. 2011. The maximum temperature of buoyancy-driven smoke flow beneath the ceiling in tunnel fires. *Fire Safety Journal* 46(4): 204-210.

Luo, M. 1997. Effects of radiation on temperature measurement in a fire environment. *Journal of Fire Sciences* 15(6): 443-461.

Mehta, R. D., & Bradshaw, P. 1979. Design rules for small low speed wind tunnels. *The Aeronautical Journal* 83(827): 443-453.

Oka, Y., & Atkinson, G. T. 1995. Control of smoke flow in tunnel fires. *Fire Safety Journal* 25(4): 305-322.

Quintiere, J. G. 1989. Scaling applications in fire research. *Fire Safety Journal* 15(1): 3-29.

Tang, F., He, Q., Chen, L., & Li, P. 2019. Experimental study on maximum smoke temperature beneath the ceiling induced by carriage fire in a tunnel with ceiling smoke extraction. *Sustainable Cities and Society* 44: 40-45.

Walker, J. D., & Stocks, B. J. 1968. Thermocouple errors in forest fire research. *Fire Technology* 4(1): 59-62.

Yan, T., Ming Heng, S., Yan Feng, G. & Jia Peng, H. 2009. Full-scale experimental study on smoke flow in natural ventilation road tunnel fires with shafts. *Tunnelling and Underground Space Technology* 24(6): 627—633.

Zhao, S., Liu, F., Wang, F., & Weng, M. 2018. Experimental studies on fire-induced temperature distribution below ceiling in a longitudinal ventilated metro tunnel. *Tunnelling and Underground Space Technology* 72: 281-293.